Journal of Sound and Vibration (1999) **228**(5), 939–959
Article No. jsvi.1998.2472, available online at http://www.idealibrary.com on IDEAL®

PARTIAL FEEDBACK LINEARIZATION ON A HARMONICALLY EXCITED BEAM WITH ONE-SIDED SPRING

M. F. HEERTJES, M. J. G. VAN DE MOLENGRAFT AND H. NIJMEIJER†

Faculty of Mechanical Engineering, Eindhoven University of Technology, P.O. Box 513, 5600 *MB Eindhoven, The Netherlands*

(*Received* 21 *December* 1998)

Partial feedback linearization is applied to a harmonically excited beam with one-sided spring to reduce vibration amplitudes while keeping the control effort small. Vibration amplitudes are reduced by globally stabilizing the small amplitude 1-periodic solution which is one of the coexisting solutions. As the 1-periodic solution represents a natural solution of the uncontrolled system, no control effort will be needed once the system vibrates in the 1-periodic response. To control the multi-degree-of-freedom (d.o.f.) beam system to the 1-periodic solution, only one actuator is used that controls one (d.o.f.). The behaviour of the other d.o.f.s is eventually described by the zero dynamics. Whether these d.o.f.s converge to the 1-periodic solution depends on the stability of the zero dynamics. The global asymptotic stability of the non-autonomous zero dynamics can be partially determined by a frequency domain technique known as the circle criterion. However, the circle criterion does not guarantee stability at all actuator positions along the beam

1. INTRODUCTION

Frequently, non-linear dynamical systems such as suspension bridges [1], gear boxes [2], or ships colliding at fenders [3], possessing several different periodic solutions at the same values for the system parameters occur. Some of these so-called coexisting periodic solutions appear as large-amplitude vibrations which can cause damage and increasing wear to the system. Stabilizing one of the coexisting periodic solutions with small-amplitude vibration can prevent damage and wear while the control effort can be kept small because once the system vibrates in the low-amplitude response no further control effort is needed.

Much effort has been made to stabilize periodic solutions embedded within chaotic attractors [4, 5], mainly because almost any small neighbourhood around any point in the attractor will be reached in finite time such that a control scheme based on a linear approximation of the system dynamics can be used to stabilize

†Also at: Faculty of Mathematical Sciences, University of Twente, P.O. Box 217, 7500 AE Enschede, The Netherlands.

0022-460X/99/500939 + 21 $30.00/0

a desired periodic solution [6, 7]. In many mechanical applications, chaotic attractors only exist in a few small regions of the parameter space, whereas damage and wear to such systems can occur in many large regions as a result of large-amplitude periodic vibrations [8]. If no chaotic attractors exist, other control schemes are needed to stabilize one of the coexisting small-amplitude periodic solutions to obtain vibration amplitude reduction [9, 10]. In this paper, non-linear control based on feedback linearization [11] will be used. Partial feedback linearization is applied because only part of the dynamics can be linearized by feedback as a result of under-actuation [12]. Under-actuation is inherent to many practical applications and occurs whenever there are less actuators than d.o.f.s.

Partial feedback linearization is used to control one actuator position on a harmonically excited beam with a one-sided spring; only if the actuator is placed at the middle of the beam, opposite to the one-sided spring, the dynamics can entirely be linearized by feedback. The actuator position is controlled from a large-amplitude 2-periodic response to a small-amplitude 1-periodic response both in simulations and experiments. At the 1-periodic response, vibration amplitudes are reduced whereas the control effort converges to zero whenever the so-called zero dynamics are globally asymptotically stable. Global asymptotic stability of the zero dynamics can be proved by applying the circle criterion [13]. However, the circle criterion guarantees stability only at certain actuator positions along the beam.

2. BEAM WITH ONE-SIDED SPRING

The harmonically excited beam with one-sided spring captures three essential elements that characterize many non-linear dynamical systems in engineering practice; see Figure 1. Firstly, it contains a beam, a large flexible structure that is supported by leaf springs and can be accurately modelled applying a linear multi-d.o.f. model. Secondly, it contains a one-sided spring, a non-smooth local non-linearity that adds a restoring force to the middle of the beam for positive displacements q_{mid} [14, 15]. Thirdly, it contains a harmonic exciter represented by a rotating mass unbalance that adds a sine-shaped force to the middle of the beam.

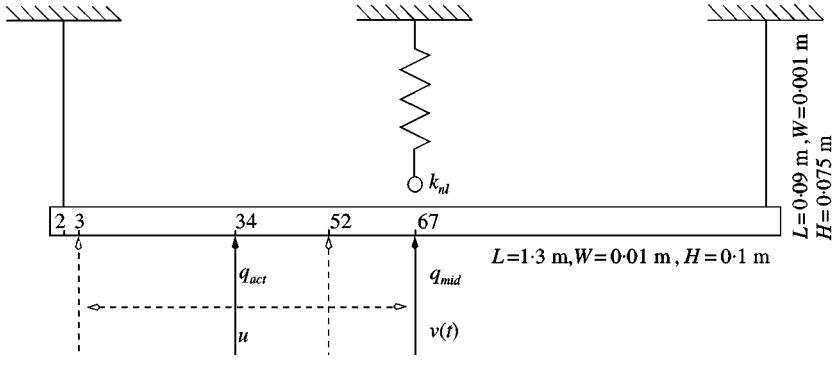

Figure 1. Beam with one-sided spring.

A simple, though, sufficiently accurate model of the beam is required for control design. A 3-d.o.f. model is obtained after reducing an accurate model with 152 d.o.f.s applying a component-mode synthesis method [16]. The 152 d.o.f. model is reduced to avoid large computational times both in simulations and experiments. The reduced model is, of course, less accurate. However, the loss of accuracy mainly applies to the high-frequency behaviour of the linear beam while our interest focuses on the low-frequency response of the non-linear beam system. The 3-d.o.f. model contains two interface d.o.f.s (q_{act}, q_{mid}) needed to apply the external forces caused by the exciter $v(t)$, the one-sided spring $F_{nl}(q)$, and the input u. Furthermore, it contains one virtual d.o.f. (q_ξ) that accounts for the first eigenmode of the beam [17]. The 3-d.o.f. model contains three positive-definite matrices: a mass matrix M, a damping matrix B, and a stiffness matrix K. These matrices depend on the position where the input u is applied. In the sequel, the input can be applied at one of the equidistantly distributed positions between the leaf spring, position 2, and the middle of the beam, position 67, see Figure 1. Initially, the input is applied at a quarter of the beam, position 34. If the actuator position is changed, the values for M, B, and K change.

The 3-d.o.f. model together with the external forces determine the equations of motion of the non-linear beam system and can be given as

$$\mathbf{M}\ddot{\mathbf{q}} + \mathbf{B}\dot{\mathbf{q}} + \mathbf{K}\mathbf{q} + \mathbf{F}_{nl}(q) = \mathbf{h}_2 v(t) + \mathbf{h}_1 u, \tag{1}$$

with the excitation force $v(t)$ represented by a known function of time

$$v(t) = A_{exc}\cos(2\pi f_{exc} t), \tag{2}$$

and the restoring force of the one-sided spring $F_{nl}(q)$ given by

$$F_{nl}(q) = k_{nl}\varepsilon(q_{mid})\mathbf{h}_2\mathbf{h}_2^{\mathrm{T}} q,\ \varepsilon(q_{mid}) = \begin{cases} 1 & \text{if } q_{mid} > 0, \\ 0 & \text{if } q_{mid} \leqslant 0, \end{cases} \tag{3}$$

with $\mathbf{q}^{\mathrm{T}} = [q_{act} \quad q_{mid} \quad q_\xi]^{\mathrm{T}}$, where h_i represents a 3×1 transition matrix with zeros except for the ith entry which equals one, A_{exc} represents the amplitude of the excitation force, f_{exc} represents the excitation frequency, and k_{nl} represents the stiffness of the one-sided spring; see Appendix A for numerical values of a 3-d.o.f. model. The equations of motion are written in state-space form as

$$\dot{\mathbf{x}} = \mathbf{A}(\mathbf{x})\mathbf{x} + \mathbf{b}_2 v(t) + \mathbf{b}_1 u = \mathbf{f}(t, \mathbf{x}) + \mathbf{b}_1 u, \tag{4}$$

with $\mathbf{x} = [\mathbf{q}^{\mathrm{T}}\dot{\mathbf{q}}^{\mathrm{T}}]^{\mathrm{T}}$, and

$$\mathbf{A}(\mathbf{x}) = \begin{bmatrix} 0 & I \\ -\mathbf{M}^{-1}(\mathbf{K} + k_{nl}\varepsilon(q_{mid})\mathbf{h}_2\mathbf{h}_2^{\mathrm{T}}) & -\mathbf{M}^{-1}\mathbf{B} \end{bmatrix}, \qquad b_i = \begin{bmatrix} 0 \\ -\mathbf{M}^{-1}\mathbf{h}_i \end{bmatrix}. \tag{5}$$

The accuracy of the model of the beam system is shown in Figure 2 for a 2-periodic solution at an excitation frequency of 35 Hz. In Figure 2, both the measured displacement, reconstructed velocity, and measured acceleration at the actuator position (q_{act}, $\dot{q}_{act}$, $\ddot{q}_{act}$), and at the middle of the beam (q_{mid}, $\dot{q}_{mid}$, $\ddot{q}_{mid}$), are depicted together with the numerical results; the velocities were reconstructed from the measured displacement and accelerations applying a switching extended Kalman

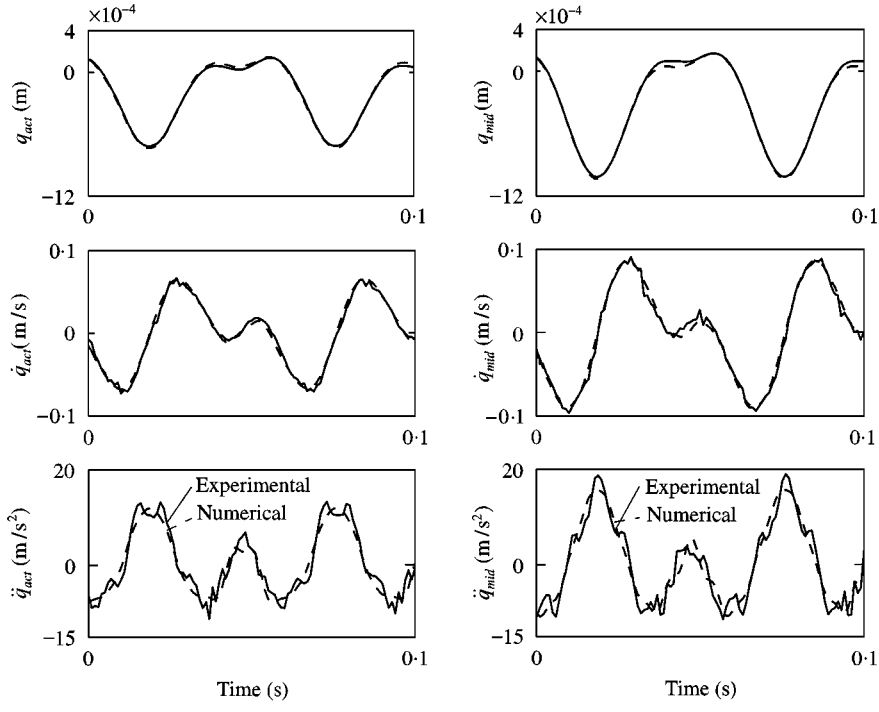

Figure 2. 2-periodic solutions of the uncontrolled beam system ($u = 0$) with an actuator placed at position 34.

filter based on the two linear regimes of the beam system: $q_{mid} > 0$, and $q_{mid} \leqslant 0$. It can be seen that a good agreement is obtained between the measured and calculated response of the uncontrolled beam system ($u = 0$). The periodic behaviour of the uncontrolled beam system as a function of the excitation frequency is depicted in Figure 3. It shows the maximum absolute values of the periodic displacement for both the actuator position $|q_{act}|_{max}$ and the middle of the beam $|q_{mid}|_{max}$. The periodic behaviour is also shown for the linear model, thus, without the one-sided spring. There are two main differences in periodic behaviour between the linear and the non-linear model. Firstly, the natural frequencies of the linear model precede the harmonic resonance frequencies of the non-linear model due to the additional stiffness of the one-sided spring in the non-linear model. Secondly, coexisting n-periodic solutions, $n \in \{2, 3, \ldots\}$, appear for the non-linear model at certain frequencies. Figure 3 shows that if different periodic solutions coexist, the 1-periodic solution has the smallest vibration amplitude in absolute value. This supports the objective to stabilize the 1-periodic solution to obtain vibration amplitude reduction.

3. EXISTENCE OF A 1-PERIODIC SOLUTION

The existence of a 1-periodic solution at an arbitrary excitation frequency is needed for the ability to stabilize it within the entire frequency domain; Figure 3 is

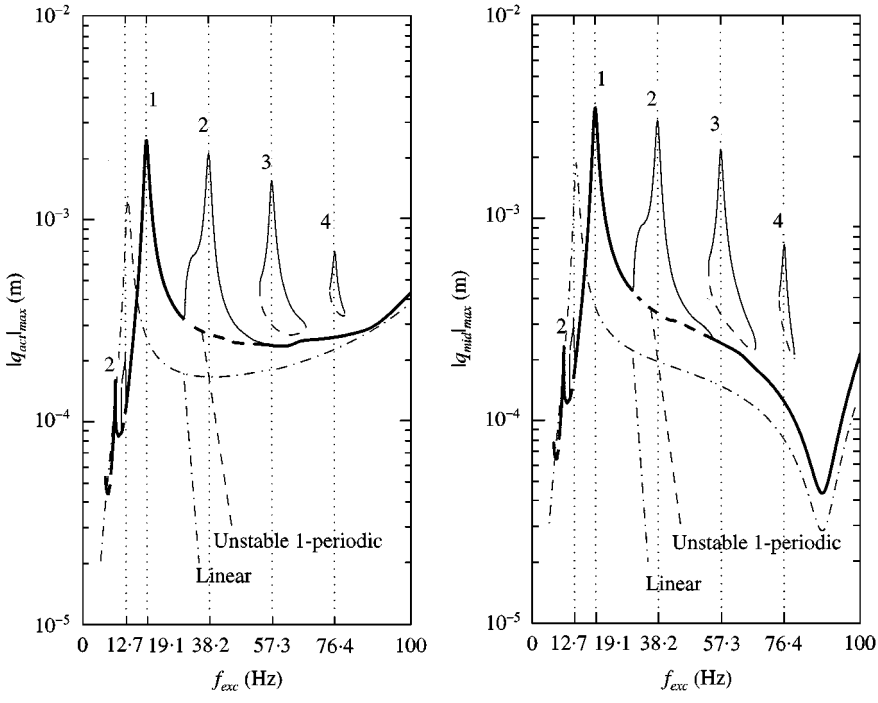

Figure 3. Periodic behaviour of the uncontrolled beam system ($u = 0$) with an actuator placed at position 34.

only an indication that such a solution indeed exists. The existence of a 1-periodic solution can be proved applying Yoshizawa's theorem [18].

Theorem. *Let* $\dot{\mathbf{x}} = \mathbf{f}(t, \mathbf{x}) = f(t + T, \mathbf{x})$ *denote the uncontrolled dynamics of the beam. Assume that, for any initial condition* $\mathbf{x}(t_0) = \mathbf{x}_0$, *these dynamics have a unique solution, and assume moreover that the solutions are ultimately bounded with bound* $\mathscr{B}$. *Then there exists a periodic solution* $\mathbf{x}$ *of period* T *such that* $\|\mathbf{x}\| \leqslant \mathscr{B}, \forall t \in R$; $\|\mathbf{X}\|$ *denotes the Euclidean norm of matrix* $\mathbf{X}$, *or* $\|\mathbf{X}\| = \sqrt{\lambda_{max}(\mathbf{X}^{\mathrm{T}}\mathbf{X})}$ *with the maximal eigenvalue of* $\mathbf{X}^{\mathrm{T}}\mathbf{X}$.

Yoshizawa's theorem exploits Browder's fixed point theorem, and requires two conditions to be fulfilled: uniqueness of solutions and ultimate boundedness.

Uniqueness of solutions can be proved if $f(t, x)$ determined via equation (4) satisfies a global Lipschitz condition. A global Lipschitz condition for the beam system can be obtained if it can be shown that $\mathbf{x}$ will always be in a set where $\mathbf{f}(t, \mathbf{x})$ is uniformly Lipschitz in $\mathbf{x}$ [19]. To ensure this, two conditions need to be fulfilled. Firstly, $\mathbf{f}(t, \mathbf{x})$ should be uniformly Lipschitz in $\mathbf{x}$, or

$$\|\mathbf{f}(t, \mathbf{x}) - \mathbf{f}(t, \mathbf{y})\| = \|\mathbf{A}(\mathbf{x})\mathbf{x} - \mathbf{A}(\mathbf{y})\mathbf{y}\|$$

$$\leqslant \mathscr{L}\|\mathbf{x} - \mathbf{y}\|, \forall \mathbf{x}, \mathbf{y} \in R^n \text{ and } \forall t \in [t_0, t_1], \tag{6}$$

with the so-called Lipschitz constant $\mathscr{L}$. For the beam system, $\mathscr{L}$ is given by

$$\mathscr{L} = \left\| \begin{bmatrix} \mathbf{0} & \mathbf{I} \\ -\mathbf{M}^{-1}(\mathbf{K} + k_{nl}\mathbf{h}_2\mathbf{h}_2^{\mathrm{T}}) & -\mathbf{M}^{-1}\mathbf{B} \end{bmatrix} \right\|. \tag{7}$$

Secondly, for each finite $\mathbf{x}(t_0) = \mathbf{x}_0$ there should exist a positive constant $h = h(\mathbf{x}_0)$ such that

$$\begin{aligned} \|\mathbf{f}(t, \mathbf{x}_0)\| &= \|\mathbf{A}(\mathbf{x}_0)\mathbf{x}_0 + \mathbf{b}_2 v(t)\| \leqslant \mathscr{L}\|\mathbf{x}_0\| + \|\mathbf{b}_2 A_{exc}\cos(2\pi f_{exc} t)\| \\ &\leqslant \mathscr{L}\|\mathbf{x}_0\| + \|\mathbf{b}_2 A_{exc}\| \leqslant h, \ \forall t \in [t_0, t_1]. \end{aligned} \tag{8}$$

As both conditions are fulfilled for the beam system whereas t_1 in equations (6) and (8) can be chosen arbitrarily large, $\mathbf{f}(t, \mathbf{x})$, which is piecewise continuous in t, can be proved to satisfy a global Lipschitz condition [19] which results in the fact that there exists a unique solution for $\dot{\mathbf{x}} = \mathbf{f}(t, \mathbf{x})$ with $\mathbf{x}(t_0) = \mathbf{x}_0$ over $[t_0, t_1]$ for all $t_1 > t_0$.

Ultimate boundedness can be proved with Khalil's lemma on non-vanishing perturbations [19]. For the application of this lemma, two conditions need to be fulfilled. Firstly, the homogeneous system, i.e., $\dot{\mathbf{x}} = \mathbf{A}(\mathbf{x})\mathbf{x}$, see equation (4), must be exponentially stable at the equilibrium point $\mathbf{x} = \mathbf{0}$. Secondly, the perturbation $\mathbf{b}_2 v(t)$ must be uniformly bounded.

Exponential stability for the homogeneous system can be shown with the following Lyapunov function candidate:

$$\begin{aligned} V(\mathbf{q}, \dot{\mathbf{q}}) = {} & \tfrac{1}{2}\dot{\mathbf{q}}^{\mathrm{T}}\mathbf{M}\dot{\mathbf{q}} + \tfrac{1}{2}(\dot{\mathbf{q}}^{\mathrm{T}} + \mathbf{q}^{\mathrm{T}})\mathbf{M}(\dot{\mathbf{q}} + \mathbf{q}) + \mathbf{q}^{\mathrm{T}}(\mathbf{K} + \tfrac{1}{2}(\mathbf{B} - \mathbf{M}))\mathbf{q} \\ & + \mathbf{q}^{\mathrm{T}} k_{nl}\varepsilon(q_{mid})\mathbf{h}_2\mathbf{h}_2^{\mathrm{T}} q, \end{aligned} \tag{9}$$

which represents an energy-like function that does not need to have a physical meaning besides the fact that $V(\mathbf{q}, \dot{\mathbf{q}})$ as a whole should be positive definite. A sufficient condition for $V(\mathbf{q}, \dot{\mathbf{q}})$ to be positive definite is obtained if $\mathbf{K} + 1/2(\mathbf{B} - \mathbf{M}) \geqslant 0$ because $\mathbf{M} = \mathbf{M}^{\mathrm{T}} > 0$, $\mathbf{B} = \mathbf{B}^{\mathrm{T}} > 0$, $\mathbf{K} = \mathbf{K}^{\mathrm{T}} > 0$, and $k_{nl}\mathbf{h}_2\mathbf{h}_2^{\mathrm{T}} = (k_{nl}\mathbf{h}_2\mathbf{h}_2^{\mathrm{T}})^{\mathrm{T}} \geqslant 0$. $V(\mathbf{q}, \dot{\mathbf{q}})$ is bounded by positive-definite quadratic functions, or

$$L_1(\mathbf{q}, \dot{\mathbf{q}}) \leqslant V(\mathbf{q}, \dot{\mathbf{q}}) \leqslant L_2(\mathbf{q}, \dot{\mathbf{q}}), \tag{10}$$

with

$$\begin{aligned} L_1(\mathbf{q}, \dot{\mathbf{q}}) &= \tfrac{1}{2}\dot{\mathbf{q}}^{\mathrm{T}}\mathbf{M}\dot{\mathbf{q}} + \tfrac{1}{2}(\dot{\mathbf{q}}^{\mathrm{T}} + \mathbf{q}^{\mathrm{T}})\mathbf{M}(\dot{\mathbf{q}} + \mathbf{q}) + \mathbf{q}^{\mathrm{T}}(\mathbf{K} + \tfrac{1}{2}(\mathbf{B} - \mathbf{M}))\mathbf{q} \\ &\geqslant \tfrac{1}{2}\dot{\mathbf{q}}^{\mathrm{T}}\mathbf{M}\dot{\mathbf{q}} + \tfrac{1}{2}(\dot{\mathbf{q}}^{\mathrm{T}} + \mathbf{q}^{\mathrm{T}})\mathbf{M}(\dot{\mathbf{q}} + \mathbf{q}) = \tfrac{1}{2}\mathbf{x}^{\mathrm{T}}\begin{bmatrix} \mathbf{M} & \mathbf{M} \\ \mathbf{M} & 2\mathbf{M} \end{bmatrix} x = \tfrac{1}{2}\mathbf{x}^{\mathrm{T}}\mathbf{M}^*\mathbf{x} \\ &\geqslant c_1\|\mathbf{x}\|^2, \end{aligned} \tag{11}$$

$$\begin{aligned} L_2(\mathbf{q}, \dot{\mathbf{q}}) &= L_1(\mathbf{q}, \dot{\mathbf{q}}) + \mathbf{q}^{\mathrm{T}} k_{nl}\mathbf{h}_2\mathbf{h}_2^{\mathrm{T}}\mathbf{q} \\ &\leqslant c_2\|\mathbf{x}\|^2. \end{aligned} \tag{12}$$

The positive constants c_1 and c_2 equal

$$c_1 = \tfrac{1}{2}\lambda_{min}(\mathbf{M}^*), \tag{13}$$

$$c_2 = \tfrac{3}{2}\|\mathbf{M}\| + \|\mathbf{K}\| + \tfrac{1}{2}\|\mathbf{B} - \mathbf{M}\| + k_{nl}, \tag{14}$$

with λ_{min} the minimal eigenvalue of the corresponding matrix. For the derivative of $V(\mathbf{q}, \dot{\mathbf{q}})$,

$$\begin{aligned}\dot{V}(\mathbf{q}, \dot{\mathbf{q}}) &= -\mathbf{q}^{\mathrm{T}}\mathbf{K}\mathbf{q} - \dot{\mathbf{q}}^{\mathrm{T}}(2\mathbf{B} - \mathbf{M})\dot{\mathbf{q}} - \mathbf{q}^{\mathrm{T}}k_{nl}\varepsilon(\mathbf{q}_{mid})\mathbf{h}_2\mathbf{h}_2^{\mathrm{T}}\mathbf{q} \\ &\leqslant -\mathbf{q}^{\mathrm{T}}\mathbf{K}\mathbf{q} - \dot{\mathbf{q}}^{\mathrm{T}}(2\mathbf{B} - \mathbf{M})\dot{\mathbf{q}} = -\mathbf{x}^{\mathrm{T}}\begin{bmatrix}\mathbf{K} & \mathbf{0} \\ \mathbf{0} & 2\mathbf{B} - \mathbf{M}\end{bmatrix}\mathbf{x} \\ &\leqslant -c_3\|\mathbf{x}\|^2\end{aligned} \tag{15}$$

holds with positive constant $c_3 = \min(\lambda_{min}(\mathbf{K}), \lambda_{min}(2\mathbf{B} - \mathbf{M}))$, $\dot{V}(\mathbf{q}, \dot{\mathbf{q}})$ is negative definite provided that $(2\mathbf{B} - \mathbf{M})$ is positive definite. Both conditions $(2\mathbf{B} - \mathbf{M}) > 0$ and $\mathbf{K} + 1/2(\mathbf{B} - \mathbf{M}) \geqslant 0$, are satisfied for the beam system at hand. Substitution of $V(\mathbf{q}, \dot{\mathbf{q}}) \leqslant c_2\|\mathbf{x}\|^2$, equation (10), gives

$$\dot{V}(\mathbf{q}, \dot{\mathbf{q}}) \leqslant -\frac{c_3}{c_2}V(\mathbf{q}, \dot{\mathbf{q}}). \tag{16}$$

This yields

$$V(\mathbf{q}, \dot{\mathbf{q}}) \leqslant V(\mathbf{q}(t_0), \dot{\mathbf{q}}(t_0))\mathrm{e}^{-(c_3/c_2)(t-t_0)}, \ \forall t \geqslant t_0, \tag{17}$$

that assures the equilibrium point $\mathbf{x} = 0$ of the homogeneous system to be exponentially stable, or

$$\|\mathbf{x}(t)\| \leqslant \sqrt{\frac{c_2}{c_1}}\,\mathrm{e}^{-(c_3/2c_2)(t-t_0)}\|\mathbf{x}(t_0)\|, \ \forall t \geqslant t_0, \tag{18}$$

because $c_1\|\mathbf{x}\|^2 \leqslant V(\mathbf{q}, \dot{\mathbf{q}}) \leqslant c_2\|\mathbf{x}\|^2$. Exponential stability for the homogeneous system results in ultimate boundedness of the perturbed system, i.e., the homogeneous system together with the perturbation $\mathbf{b}_2 v(t)$, if the perturbation is uniformly bounded at an arbitrary excitation frequency, or

$$\|\mathbf{b}_2 v(t)\| = \|\mathbf{b}_2 A_{exc}\cos(2\pi f_{exc}t)\| \leqslant \|\mathbf{b}_2 A_{exc}\| = c_4, \ \forall t \geqslant 0. \tag{19}$$

This can be seen as follows. If $V(\mathbf{q}, \dot{\mathbf{q}})$ in equation (9) is used as a Lyapunov function candidate for the perturbed system, the following upper bound can be obtained on the derivative $\dot{V}(\mathbf{q}, \dot{\mathbf{q}})$,

$$\begin{aligned}\dot{V}(\mathbf{q}, \dot{\mathbf{q}}) &\leqslant -c_3\|\mathbf{x}\|^2 - \frac{\partial V(\mathbf{q}, \dot{\mathbf{q}})}{\partial \dot{\mathbf{q}}}\mathbf{M}^{-1}\mathbf{h}_2 v(t) \\ &\leqslant -c_3\|\mathbf{x}\|^2 + \left\|\frac{\partial V(\mathbf{q}, \dot{\mathbf{q}})}{\partial \dot{\mathbf{q}}}\right\| c_4 \\ &\leqslant -c_3\|\mathbf{x}\|^2 + c_4 c_5\|\mathbf{x}\|,\end{aligned} \tag{20}$$

since for the partial derivative of $V(\mathbf{q}, \dot{\mathbf{q}})$,

$$\left\| \frac{\partial V(\mathbf{q}, \dot{\mathbf{q}})}{\partial \dot{\mathbf{q}}} \right\| = \|2\mathbf{M}\dot{\mathbf{q}} - \mathbf{M}\mathbf{q}\| \leqslant 3\|\mathbf{M}\|\|\mathbf{x}\| = c_5\|\mathbf{x}\| \tag{21}$$

holds. This upper bound on $\dot{V}(\mathbf{q}, \dot{\mathbf{q}})$ can be written as

$$\dot{V}(\mathbf{q}, \dot{\mathbf{q}}) \leqslant -(1-\theta)c_3\|\mathbf{x}\|^2 - \theta c_3\|\mathbf{x}\|^2 + c_4c_5\|\mathbf{x}\|, \tag{22}$$

with $0 < \theta < 1$. It follows that for all $\|\mathbf{x}\| \geqslant (c_4c_5)/(\theta c_3)$, $\dot{V}(\mathbf{q}, \dot{\mathbf{q}})$ is negative definite. In other words, all solutions of equation (20) are ultimately confined to the region $\|\mathbf{x}\| < (c_4c_5)/(\theta c_3)$ because here

$$\dot{V}(\mathbf{q}, \dot{\mathbf{q}}) \leqslant -(1-\theta)c_3\|\mathbf{x}\|^2, \forall \|\mathbf{x}\| \geqslant \frac{c_4c_5}{\theta c_3} \tag{23}$$

holds. Substitution of $V(\mathbf{q}, \dot{\mathbf{q}}) \leqslant c_2\|\mathbf{x}\|^2$, gives

$$\dot{V}(\mathbf{q}, \dot{\mathbf{q}}) \leqslant -(1-\theta)\frac{c_3}{c_2}V(\mathbf{q}, \dot{\mathbf{q}}), \forall \|\mathbf{x}\| \geqslant \frac{c_4c_5}{\theta c_3}. \tag{24}$$

This results in the following behaviour for $\|\mathbf{x}\|$,

$$\|\mathbf{x}(t)\| \leqslant \sqrt{\frac{c_2}{c_1}}\, e^{-(1-\theta)(c_3/2c_2)(t-t_0)}\|\mathbf{x}(t_0)\|, \forall \|\mathbf{x}\| \geqslant \frac{c_4c_5}{\theta c_3}, t_0 \leqslant t < t_1, \tag{25}$$

as $c_1\|\mathbf{x}\|^2 \leqslant V(\mathbf{q}, \dot{\mathbf{q}}) \leqslant c_2\|\mathbf{x}\|^2$. So, far all $\|\mathbf{x}\| \geqslant (c_4c_5)/(\theta c_3)$, $\|\mathbf{x}\|$ is bounded by a function that decreases exponentially. Therefore, $\|\mathbf{x}\|$ is ultimately bounded by the value of this function at $\|\mathbf{x}\| = (c_4c_5)/(\theta c_3)$, or

$$\|\mathbf{x}(t)\| \leqslant \sqrt{\frac{c_2}{c_1}} \times 1 \times \frac{c_4c_5}{\theta c_3} = \mathscr{B}, \forall t \geqslant t_1. \tag{26}$$

It can be concluded that for any finite $\mathbf{x}(t_0)$, the solution $\mathbf{x}$ of the uncontrolled beam system will remain below the positive constant $\mathscr{B}$ after some finite time t_1.

Ultimate boundedness combined with the existence and uniqueness of solutions enables the application of Yoshizawa's theorem which guarantees the existence of a 1-periodic solution for the uncontrolled beam system. The existence of a 1-periodic solution p justifies the study of the error dynamics related to this solution which is used in the control design based on feedback linearization.

4. PARTIAL FEEDBACK LINEARIZATION

Feedback linearization [11] can be applied to control the beam system as an accurate model is available. The multi-d.o.f. beam system is controlled with only one actuator, i.e., the controlled system is under-actuated. Due to under-actuation, only part of the system dynamics can be linearized by feedback. Therefore, a version of partial feedback linearization is applied which linearizes that part of the dynamics needed to guarantee the actuator position to vibrate in the 1-periodic response. For the special case where the actuator is placed at the middle of the

beam, opposite to the one-sided spring, the entire dynamics can be linearized by feedback. This enables a version of feedback linearization that compensates only for the non-linear terms resulting in the control effort to be zero part of the time.

Both feedback linearization and partial feedback linearization will be applied to the error dynamics of the beam system. The error dynamics are obtained by subtracting the equations of motion of the 1-periodic solution $\mathbf{p}$, $\mathbf{p} = [p_{act} \quad p_{mid} \quad p_\xi]^T$, from the equations of motion at the momentary solution $\mathbf{q}$, see equation (1), or

$$\mathbf{M}\ddot{\mathbf{e}} + \mathbf{B}\dot{\mathbf{e}} + \mathbf{K}\mathbf{e} + \mathbf{h}_2\phi(t, e_{mid}) = \mathbf{h}_1 u, \tag{27}$$

with $\mathbf{e} = \mathbf{q} - \mathbf{p} = [e_{act} \quad e_{mid} \quad e_\xi]^T$, and

$$\phi(t, e_{mid}) = k_{nl}\varepsilon(q_{mid})q_{mid} - k_{nl}\varepsilon(p_{mid})p_{mid}. \tag{28}$$

A special feature of these error dynamics, which will be exploited in the stability analysis in the next section, is the sector-bounded non-linearity $\phi(t, e_{mid})$ for which

$$0 \leqslant \Phi(t, e_{mid}) = \frac{\phi(t, e_{mid})}{e_{mid}} \leqslant k_{nl},\ \Phi(t, 0) = 0 \tag{29}$$

holds. The sector-boundedness is depicted in Figure 4 for two periodic solutions of the error dynamics with $u = 0$: a 2-periodic solution at 38 Hz, and a 3-periodic solution at 57 Hz. It can be seen that $\Phi(t, e_{mid})$ remains bounded by $[0, k_{nl}]$; note that $\Phi(t, e_{mid})$ is periodic with a fundamental frequency ω_f of 19 Hz.

Partial feedback linearization is applied with an actuator placed at an arbitrary position along the beam where the dynamics can only be partially linearized by feedback. In this case, the input u is chosen as

$$u = \frac{1}{\mathbf{h}_1^T\mathbf{M}^{-1}\mathbf{h}_1}\{\mathbf{h}_1^T\mathbf{M}^{-1}(\mathbf{B}\dot{\mathbf{e}} + \mathbf{K}\mathbf{e} + \mathbf{h}_2\phi(t, e_{mid})) + \omega\}. \tag{30}$$

The first part of u compensates part of the error dynamics whereas the second part consists of a new input w. This input is chosen such that a desired behaviour for the actuator position is obtained, or

$$w = -K_D\dot{e}_{act} - K_P e_{act}, \tag{31}$$

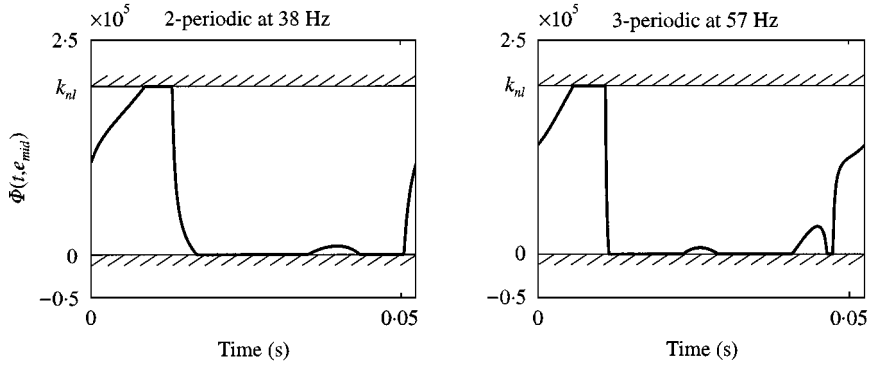

Figure 4. Sector-bounded non-linearity $\Phi(t, e_{mid})$ of the uncontrolled beam system ($u = 0$) for a 2-periodic solution at 38 Hz and a 3-periodic solution at 57 Hz.

where K_P and K_D are positive control parameters. The feedback (30, 31) transforms the error dynamics of equation (27) into

$$\ddot{e}_{act} + K_D \dot{e}_{act} + K_P e_{act} = 0, \tag{32}$$

for the d.o.f. at the actuator position, and

$$\mathbf{M}_{in}\ddot{\mathbf{e}} + \mathbf{B}_{in}\dot{\mathbf{e}} + \mathbf{K}_{in}\mathbf{e} + \mathbf{h}_{in}\phi(t, e_{mid}) = 0, \tag{33}$$

with $\mathbf{h}_{in} = [1 \quad 0]^{\mathrm{T}}$, $\mathbf{M}_{in} = \mathbf{L}_{in}\mathbf{M}$, $\mathbf{B}_{in} = \mathbf{L}_{in}\mathbf{B}$, $\mathbf{K}_{in} = \mathbf{L}_{in}\mathbf{K}$, and $\mathbf{L}_{in} = [h_2 \quad h_3]^{\mathrm{T}}$, for the so-called internal dynamics which are assumed to have a bounded solution. Equation (32) is globally asymptotically stable at $e_{act} = \dot{e}_{act} = 0$ using Lyapunov's second method with the Lyapunov function candidate $V_{PFL}(e_{act}, \dot{e}_{act})$:

$$V_{PFL}(e_{act}, \dot{e}_{act}) = \tfrac{1}{2}\dot{e}_{act}^2 + \tfrac{1}{2}K_P e_{act}^2,$$

$$\dot{V}_{PFL}(e_{act}, \dot{e}_{act}) = -K_D \dot{e}_{act}^2. \tag{34}$$

As $\dot{V}_{PFL}(e_{act}, \dot{e}_{act})$ is only negative semi-definite in the state $(e_{act}, \dot{e}_{act})$, it is necessary to determine the largest invariant set in $\{(e_{act}, \dot{e}_{act}) \in R^2 \,|\, \dot{V}_{PFL}(e_{act}, \dot{e}_{act}) = 0\}$. For the beam system, this set equals the origin. Therefore, the global asymptotic stability at $e_{act} = \dot{e}_{act} = 0$ is guaranteed after using LaSalle's theorem [19]. When $(e_{act}, \dot{e}_{act})$ tends to zero, the internal dynamics of equation (33) is no longer influenced by e_{act} and is now called the zero dynamics. The zero dynamics is defined to be the internal dynamics of the beam system when the output $y = e_{act}$ is kept at zero by the input u. The stability of the zero dynamics cannot be influenced by the control parameters K_P and K_D. Therefore, vibration reduction with small control effort depends on whether the zero dynamics converges to zero, i.e., whether the zero dynamics is globally asymptotically stable.

The special case for which the feedback linearization is applied with an actuator placed at the middle of the beam, i.e., the entire dynamics can be linearized by feedback, the controlled error dynamics of equation (27) enables the input u to be zero part of the time. For this purpose, the input only compensates the non-linear term $\phi(t, e_{mid})$, or

$$u = \frac{1}{\mathbf{h}_2^{\mathrm{T}}\mathbf{M}^{-1}\mathbf{h}_2}\{\mathbf{h}_2^{\mathrm{T}}\mathbf{M}^{-1}\mathbf{h}_2\,\phi(t, e_{mid})\} = \phi(t, e_{mid}). \tag{35}$$

As $\phi(t, e_{mid})$ equals zero in one regime of the state variable $e_{mid} = q_{mid} - p_{mid}$, the input also equals zero at this regime; see Table 1. Besides $\phi(t, e_{mid})$, also the complementary function $-\phi'(t, e_{mid})$, can be compensated by the input. The complementary function $-\phi'(t, e_{mid})$ is related to $\phi(t, e_{mid})$ by

$$\phi(t, e_{mid}) = k_{nl}e_{mid} - \phi'(t, e_{mid}). \tag{36}$$

The error equation based on each of the inputs is given by

$$\mathbf{M}\ddot{\mathbf{e}} + \mathbf{B}\dot{\mathbf{e}} + (\mathbf{K} + ik_{nl}\mathbf{h}_2\mathbf{h}_2^{\mathrm{T}})\mathbf{e} = \mathbf{0}, \quad i \in \{0, 1\}, \tag{37}$$

with $i = 0$ for the input that compensates $\phi(t, e_{mid})$ and $i = 1$ for the input that compensates $-\phi'(t, e_{mid})$. This error equation is globally asymptotically stable for

TABLE 1

Input u related to the sector-bounded non-linearity

Regime	$\phi(t, e_{mid})$	$-\phi'(t, e_{mid})$	$u = \phi(t, e_{mid})$	$u = -\phi'(t, e_{mid})$
$q_{mid} \geqslant 0, p_{mid} \geqslant 0$	$k_{nl} e_{mid}$	0	$u = k_{nl} e_{mid}$	$u = 0$
$q_{mid} \geqslant 0, p_{mid} < 0$	$k_{nl} q_{mid}$	$k_{nl} p_{mid}$	$u = k_{nl} q_{mid}$	$u = k_{nl} p_{mid}$
$q_{mid} < 0, p_{mid} \geqslant 0$	$-k_{nl} p_{mid}$	$-k_{nl} q_{mid}$	$u = -k_{nl} p_{mid}$	$u = -k_{nl} q_{mid}$
$q_{mid} < 0, p_{mid} < 0$	0	$-k_{nl} e_{mid}$	$u = 0$	$u = -k_{nl} e_{mid}$

the entire beam system $\mathbf{e} = \dot{\mathbf{e}} = \mathbf{0}$ using Lyapunov's second method with the Lyapounov function candidate $V_{FL}(\mathbf{e}, \dot{\mathbf{e}})$ for each of the inputs:

$$V_{FL}(\mathbf{e}, \dot{\mathbf{e}}) = \tfrac{1}{2}\dot{\mathbf{e}}^{\mathrm{T}} \mathbf{M} \dot{\mathbf{e}} + \tfrac{1}{2}\mathbf{e}^{\mathrm{T}}(\mathbf{K} + \mathrm{i}k_{nl}\mathbf{h}_2\mathbf{h}_2^{\mathrm{T}})\mathbf{e},\ i \in \{0, 1\},$$

$$\dot{V}_{FL}(\mathbf{e}, \dot{\mathbf{e}}) = -\dot{\mathbf{e}}^{\mathrm{T}} \mathbf{B} \dot{\mathbf{e}}. \tag{38}$$

$\dot{V}_{FL}(\mathbf{e}, \dot{\mathbf{e}})$ is negative semi-definite, but again the largest invariant set in $\{(\mathbf{e}, \dot{\mathbf{e}}) \in R^6 \mid \dot{V}_{FL}(\mathbf{e}, \dot{\mathbf{e}}) = 0\}$ equals the origin. Therefore, global asymptotic stability at the origin is guaranteed after using LaSalle's theorem.

In general, it will not be possible to choose the input u to compensate the non-linear terms. Therefore, the ability to stabilize the 1-periodic solution of the beam system will depend on the stability of the zero dynamics. To determine this stability, the circle criterion can be applied.

5. STABILITY OF THE ZERO DYNAMICS BY THE CIRCLE CRITERION

Stability proofs for non-autonomous zero dynamics that contain a non-smooth non-linearity are often related to a frequency domain technique known as the circle criterion [19]. The circle criterion can be used to guarantee the existence of a quadratic Lyapunov function which guarantees the global asymptotic stability of the zero dynamics [13]. However, for the beam system, the circle criterion guarantees this stability only for a limited range of actuator positions.

The zero dynamics of the controlled beam system is given by

$$\mathbf{M}_z \ddot{\mathbf{z}} + \mathbf{B}_z \dot{\mathbf{z}} + \mathbf{K}_z \mathbf{z} + \mathbf{h}_z \phi(t, e_{mid}) = \mathbf{0}, \tag{39}$$

with $\mathbf{z} = [e_{mid} \quad e_\xi]^{\mathrm{T}}$, $\mathbf{h}_z = [1 \quad 0]^{\mathrm{T}}$, and positive-definite matrices $\mathbf{M}_z = \mathbf{L}_z \mathbf{M} \mathbf{L}_z^{\mathrm{T}}$, $\mathbf{B}_z = \mathbf{L}_z \mathbf{B} \mathbf{L}_z^{\mathrm{T}}$, and $\mathbf{K}_z = \mathbf{L}_z \mathbf{K} \mathbf{L}_z^{\mathrm{T}}$ with $\mathbf{L}_z = [\mathbf{h}_2 \quad \mathbf{h}_3]^{\mathrm{T}}$. A state-space model for the zero dynamics is written as

$$\dot{\boldsymbol{\varepsilon}} = A_z \boldsymbol{\varepsilon} - b_z \mathbf{u},$$

$$y = \mathbf{c}_z^{\mathrm{T}} \boldsymbol{\varepsilon} = e_{mid},$$

$$u = -\phi(t, e_{mid}), \tag{40}$$

with $\boldsymbol{\varepsilon} = [z^{\mathrm{T}}\ \dot{z}^{\mathrm{T}}]^{\mathrm{T}}$, and

$$\mathbf{A}_z = \begin{bmatrix} \mathbf{0} & \mathbf{I} \\ -\mathbf{M}_z^{-1}\mathbf{K}_z & -\mathbf{M}_z^{-1}\mathbf{B}_z \end{bmatrix}, \qquad \mathbf{b}_z = \begin{bmatrix} 0 \\ -\mathbf{M}_z^{-1}\mathbf{h}_z \end{bmatrix}, \quad \mathbf{c}_z = \begin{bmatrix} h_z \\ 0 \end{bmatrix}. \tag{41}$$

This model constitutes the linear transfer between the input u and the output y, represented by the frequency response function $\chi_z(\mathrm{j}\omega)$:

$$\chi_z(\mathrm{j}\omega) = \frac{Y(\mathrm{j}\omega)}{U(\mathrm{j}\omega)} = \mathbf{c}_z^{\mathrm{T}}(\mathbf{A}_z - \mathrm{j}\omega\mathbf{I})^{-1}\mathbf{b}_z. \tag{42}$$

If $\mathbf{A}_z$ has no eigenvalues on the imaginary axis, if the non-linearity $\phi(t, e_{mid})$ is sector-bounded, and if the linear error dynamics with $u = -k_i e_{mid}$, $k_i \in [0, k_{nl}]$, is globally asymptotically stable, then the circle criterion can be applied to investigate whether $z = \dot{z} = 0$ is globally asymptotically stable [13]. The circle criterion guarantees this stability when the inequality

$$\Re\{\chi_z(\mathrm{j}\omega)\} > -\frac{1}{k_{nl}}, \ \forall\omega \in R, \tag{43}$$

is satisfied where $\Re$ denotes the real part of the corresponding function. The circle criterion is based on the linear part of the zero dynamics. This linear part differs when the complementary system description of the zero dynamics is used. The complementary system is obtained by substitution of $\phi(t, e_{mid}) = k_{nl}e_{mid} - \phi'(t, e_{mid})$, equation (36), in the state-space model of equation (40). The circle criterion applied to the complementary system gives

$$\Re\{\chi'_z(\mathrm{j}\omega)\} > -\frac{1}{k_{nl}}, \ \forall\omega \in R, \tag{43}$$

with $\chi'_z(\mathrm{j}\omega) = \mathbf{c}_z^{\mathrm{T}}(\mathbf{A}'_z - \mathrm{j}\omega\mathbf{I})^{-1}\mathbf{b}_z$ and $\mathbf{A}'_z\boldsymbol{\varepsilon} = \mathbf{A}_z\varepsilon k_{nl}\mathbf{b}_z e_{mid}$, which can give less conservative results.

The graphical representation of both inequalities (43) and (44), requires that $\chi_z(\mathrm{j}\omega)$ and $\chi'_z(\mathrm{j}\omega)$, respectively, remain to the right of the vertical line through the point $(-1/k_{nl}, 0)$ in the complex plane. This can be seen in Figure 5 where $\chi_z(\mathrm{j}\omega)$ is depicted for an actuator placed at a quarter of the beam, position 34, or closer to the middle of the beam, position 52, see Figure 1. At position 34, the global asymptotic stability of the zero dynamics cannot be proved with the circle criterion based on $\chi_z(\mathrm{j}\omega)$ because $\chi_z(\mathrm{j}\omega)$ does not remain to the right of the vertical line through the point $(-1/k_{nl}, 0)$. However, at position 52, the global asymptotic stability of the zero dynamics is proved with the circle criterion because $\chi_z(\mathrm{j}\omega)$ remains to the right of this line.

The circle criterion guarantees global asymptotic stability of the zero dynamics only for a limited range of actuator positions. This is shown in Figure 6, where the minimal real values for both frequency response functions are depicted. It can be seen that one of the frequency domain inequalities is always satisfied for actuator positions in a range between the middle of the beam, position 67, and position 50. As each of the inequalities provides a sufficient condition for global asymptotic stability, the 1-periodic solution can be stabilized globally asymptotically with one

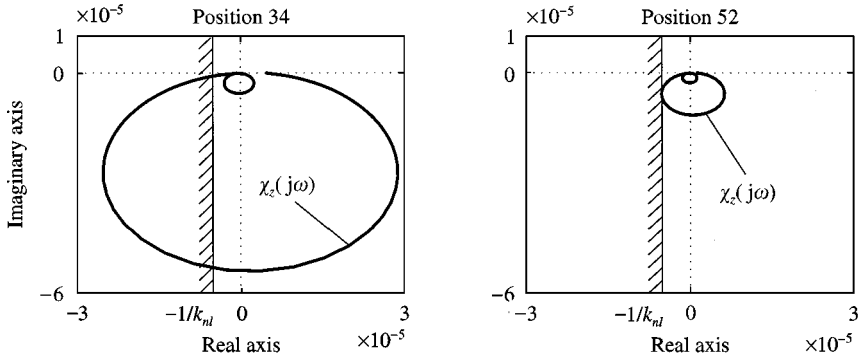

Figure 5. Graphical representation of the circle criterion for the zero dynamics with an actuator placed at position 34 and position 52 respectively.

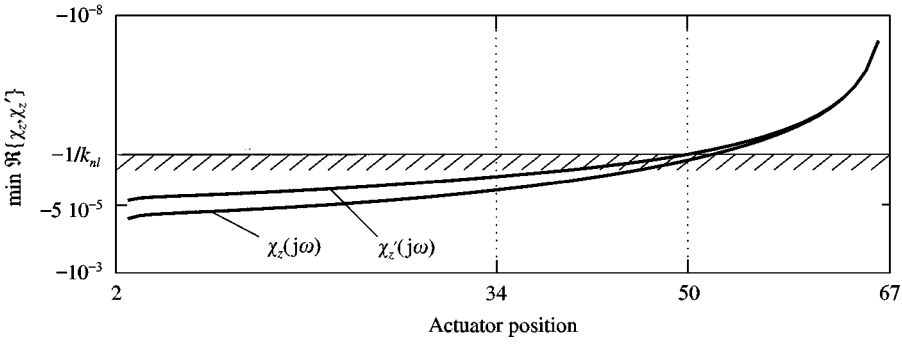

Figure 6. The circle criterion for the zero dynamics at different actuator positions along the beam.

actuator placed anywhere between position 67 and position 50. This range can be extended when the stiffness of the one-sided spring is decreased. For example, when $k_{nl} \leqslant 2 \times 10^4$ N/m, $-1/k_{nl} \leqslant -5 \times 10^{-5}$/N m, the circle criterion guarantees global asymptotic stability of the 1-periodic solution at any actuator position.

6. EXISTENCE OF PERIODIC SOLUTIONS FOR THE ZERO DYNAMICS

To possibly extend the range of actuator positions for which the 1-periodic solution of the beam system can be stabilized globally, the stability of the zero dynamics is related to the existence of periodic solutions for these dynamics. Namely, if no periodic solutions for the zero dynamics exist no quasi-periodic or chaotic solutions exist. A quasi-periodic solution is composed of a countable sum of periodic solutions, whereas a chaotic solution has embedded within it an infinite number of unstable periodic solutions [20, 21]. If no periodic, quasi-periodic, or chaotic solutions exist for the zero dynamics of the beam system besides $\mathbf{z} = \dot{\mathbf{z}} = \mathbf{0}$, consequently no bounded long-term solutions exist besides $\mathbf{z} = \dot{\mathbf{z}} = \mathbf{0}$. However, all solutions for the zero dynamics can be proved to be ultimately bounded similar to the proof obtained for the uncontrolled dynamics. Therefore, $\mathbf{z} = \dot{\mathbf{z}} = \mathbf{0}$ must be

globally asymptotically stable if no periodic solutions for the zero dynamics of the beam system exist.

Periodic solutions for the zero dynamics can only exist when the inequalities (43) and (44) from the circle criterion are not satisfied. Otherwise, the sector condition is violated which can be seen as follows. The sector condition

$$0 \leqslant \frac{\phi(t, y)}{y} \leqslant k_{nl}, \ \forall t \in R, \tag{45}$$

implies

$$-\phi(t, y)(k_{nl} y(t) - \phi(t, y)) \leqslant 0, \ \forall t \in R, \tag{46}$$

which can be shown by multiplying the sector condition with y^2, subtracting $\phi(t, y)y$ from it, and using the fact that $a \leqslant 0 \leqslant b$ implies $ab \leqslant 0$. A violation of the sector condition with $u = -\phi(t, y)$ would result in

$$\Re\{u^c u + k_{nl} u^c y\} > 0, \ \forall t \in R, \tag{47}$$

where the superscript c denotes the complex conjugate; since u is real-valued one has $u^c = u$. integration of this equation gives

$$\Re\left\{\int_0^\infty (u^c u + k_{nl} u^c y)\,\mathrm{d}t\right\} > 0. \tag{48}$$

Applying Parceval's theorem as both u and y are periodic results in

$$\Re\left\{\int_{-\infty}^{\infty} (U^c(\mathrm{j}\omega)U(\mathrm{j}\omega) + k_{nl} U^c(\mathrm{j}\omega)Y(\mathrm{j}\omega))\,\mathrm{d}\omega\right\} > 0. \tag{49}$$

Substitution of $\chi_z(\mathrm{j}\omega) = \mathbf{Y}(\mathrm{j}\omega)\mathbf{U}^{-1}(\mathrm{j}\omega)$ gives

$$\Re\left\{\int_{-\infty}^{\infty} \mathbf{U}^c(\mathrm{j}\omega)\mathbf{U}(\mathrm{j}\omega)(1 + k_{nl}\chi_z(\mathrm{j}\omega))\,\mathrm{d}\omega\right\} > 0, \tag{50}$$

which always holds if

$$\Re\{1 + k_{nl}\chi_z(\mathrm{j}\omega)\} > 0, \ \forall \omega \in R. \tag{51}$$

Inequality (51) is equal to inequality (43) used in the circle criterion. Apparently, for the beam system, the circle criterion can be interpreted being a condition for the non-existence of periodic solutions due to a violation of the sector condition. To avoid such a violation, every periodic solution for the zero dynamics should satisfy for at least one frequency ω

$$\Re\{\chi_z(\mathrm{j}\omega)\} \leqslant -\frac{1}{k_{nl}}, \quad \chi_z(\mathrm{j}\omega) = \frac{\sum_{n=-\infty}^{\infty} c_n^y \delta(\omega - n\omega_f)}{\sum_{n=-\infty}^{\infty} c_n^u \delta(\omega - n\omega_f)}, \tag{52}$$

where c_j^i denotes the jth Fourier coefficient belonging to the periodic signal i. For the individual frequency components,

$$\chi_z(\mathrm{j}n\omega_f) = \frac{Y(\mathrm{j}n\omega_f)}{U(\mathrm{j}n\omega_f)} = \frac{c_n^y}{c_n^u}, \quad n \in \{0, 1, 2, \dots\} \tag{53}$$

holds. From this equation it can be concluded that, in terms of $\chi_z(\mathrm{j}\omega)$, all n-periodic solutions, $n \in \{1, 2, \ldots\}$, with the same fundamental frequency ω_f are equal.

To show that periodic solutions for the zero dynamics, represented by $\chi_z(\mathrm{j}\omega)$, satisfy equation (52), first the uncontrolled error dynamics, represented by $\chi(\mathrm{j}\omega)$, are studied. The uncontrolled error dynamics are depicted in Figure 7 with an actuator placed at position 34. It can be seen that the 2-periodic solution at 38 Hz (○), and the 3-periodic solution at 57 Hz (∗), both based on $\omega_f = 19$ Hz, indeed have a frequency component that satisfies $\Re\{\chi(\mathrm{j}\omega)\} \leqslant -1/k_{nl}$ whereas both solutions are equal in terms of $\chi(\mathrm{j}\omega)$. In Figure 7, also the eigenvalues belonging to the homogeneous systems are depicted for both linear regimes: $\omega^i_{0,1}$ if $q_{mid} \leqslant 0$, and $\omega^i_{0,2}$ if $q_{mid} > 0$, $i \in \{1, 3\}$. It can be seen that the existence of periodic error solutions is restricted by the eigenvalues $\omega^1_{0,1}$ and $\omega^1_{0,2}$; for the considered dynamics this can be shown numerically for values of k_{nl} up to $\approx 10^7$ N/m which can be increased significantly when decreasing the modal damping. Periodic error solutions based on fundamental frequencies ω_f larger than $\omega^1_{0,2}$ would always satisfy the frequency domain inequality (51) and so they do not exist for the considered dynamics; $\Re\{\chi(\mathrm{j}\omega^1_{0,2})\}$ being almost equal to $-1/k_{nl}$ can be derived from $\Re\{\chi'(\mathrm{j}\omega^1_{0,2})\} \approx 0$ resulting from the system being proportionally damped.

The existence of periodic solutions for the zero dynamics is restricted by the eigenvalues $\omega^{*1}_{0,1}$ and $\omega^{*1}_{0,2}$ belonging to the homogeneous systems in both linear regimes of the internal dynamics; see the left part of Figure 8. However, it can be seen in the right part of Figure 8 that when the stiffness of the one-sided spring is increased to ten times its value, $10k_{nl}$, periodic solutions with fundamental frequency $\omega_f \in \{\omega^{*2}_{0,1}, \omega^{*2}_{0,2}\}$ can also exist. Furthermore, Figure 8 shows that inequality (51) is not satisfied for the current beam system with an actuator placed at position 34. Therefore, it is expected that the controlled beam system contains coexisting periodic solutions. This is shown in Figure 9, where in the left part the local asymptotic stability of the 1-periodic solution is depicted at different actuator positions and at different excitation frequencies. Local asymptotic stability of the 1-periodic solution is determined by its Floquet multipliers [20]. If all Floquet

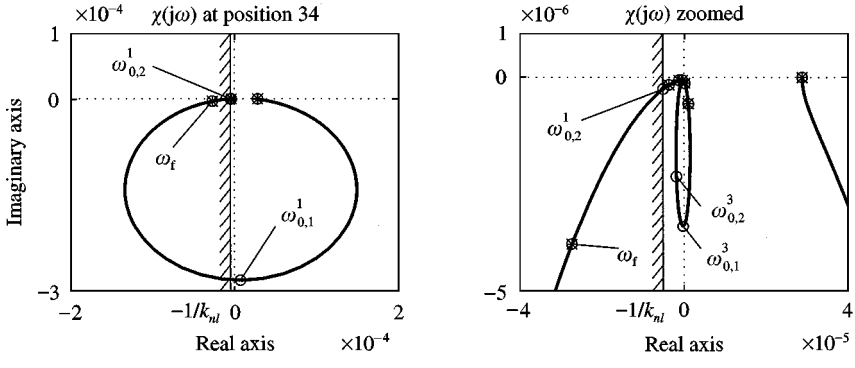

Figure 7. Existence of periodic solutions for the uncontrolled error dynamics with an actuator placed at position 34.

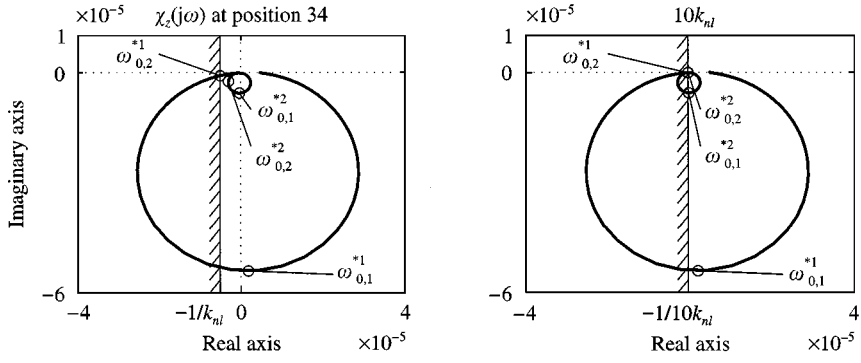

Figure 8. Existence of periodic solutions for the zero dynamics with an actuator placed at position 34.

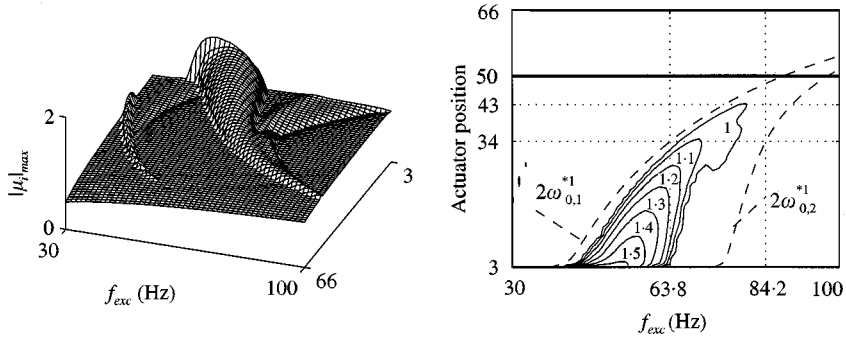

Figure 9. Local and global asymptotic stability of the zero dynamics at different actuator positions and excitation frequencies.

multipliers μ_i are less than one in absolute value, the 1-periodic solution is locally asymptotically stable. In the right part of Figure 9, it is shown that the 1-periodic solution is unstable at certain excitation frequencies for all actuator positions up to position 43. This can be seen by the lines marked 1 to 1·5 which represent lines of equal height for the largest Floquet multiplier in absolute value. As the 1-periodic solution is unstable, periodic solutions for the zero dynamics must exist. However, these periodic solutions are restricted by the eigenvalues belonging to both homogeneous systems, $\omega_{0,1}^{*i}$ and $\omega_{0,2}^{*i}$. These eigenvalues change if the actuator is placed at different positions along the beam because the positive-definite matrices $\mathbf{M}_z$, $\mathbf{B}_z$, and $\mathbf{K}_z$ change with the actuator position. For example, with an actuator placed at position 34, 2-periodic solutions with fundamental frequency ω_f, or $2\omega_f \in [2\omega_{0,1}^{*1}, 2\omega_{0,2}^{*1}]$, can exist for excitation frequencies restricted by $f_{exc} = 2\omega_{0,1}^{*1} = 63{\cdot}8$ Hz and $f_{exc} = 2\omega_{0,2}^{*1} = 84{\cdot}2$ Hz, see the right part of Figure 9. As 2-periodic solutions exist up to position 43, global asymptotic stability cannot occur below this actuator position. However, global asymptotic stability could be guaranteed with the circle criterion for actuator positions ranging from position 50 to the middle of the beam at position 67. So, if conservatism is induced when applying the circle criterion, it only occurs within a region of actuator positions between position 43 and position 50.

7. SIMULATIONS AND EXPERIMENTS

Simulations and experiments illustrate the ability to stabilize the 1-periodic solution of the beam system. Simulations are performed for two different actuator positions: at the middle of the beam, and at a quarter of the beam. At the middle of the beam, stability of the error dynamics is guaranteed for all d.o.f.s whereas the input can be kept zero part of the time. At quarter of the beam, stability is guaranteed only for the d.o.f. at the actuator position whereas the stability of the other d.o.f.s depends on the stability of the zero dynamics. To illustrate the ability to stabilize the 1-periodic solution in case only local asymptotic stability for the zero dynamics can be obtained, experiments are performed with an actuator placed at this position.

Feedback linearization applied at the middle of the beam guarantees global asymptotic stability at $\mathbf{e} = \dot{\mathbf{e}} = \mathbf{0}$ for the entire beam system whereas the input u can be kept zero part of the time. This is shown in Figure 10, by simulations, where the input is chosen to compensate the sector-bounded non-linearity: $u = \phi(t, e_{mid})$ in the left part, and $u = -\phi'(t, e_{mid})$ in the right part. With these inputs, all d.o.f.s starting from the large-amplitude 2-periodic solution at 37 Hz converge to the small-amplitude 1-periodic solution after control is switched on at $t = 0{\cdot}5$ s. Stabilizing the 1-periodic solution results in vibration amplitude reduction as seen in the upper part of Figure 10 where q_{act} is depicted. The corresponding control effort converges to zero as the errors converge to zero as seen in the lower part of Figure 10. The error convergence is similar for both inputs because the damping

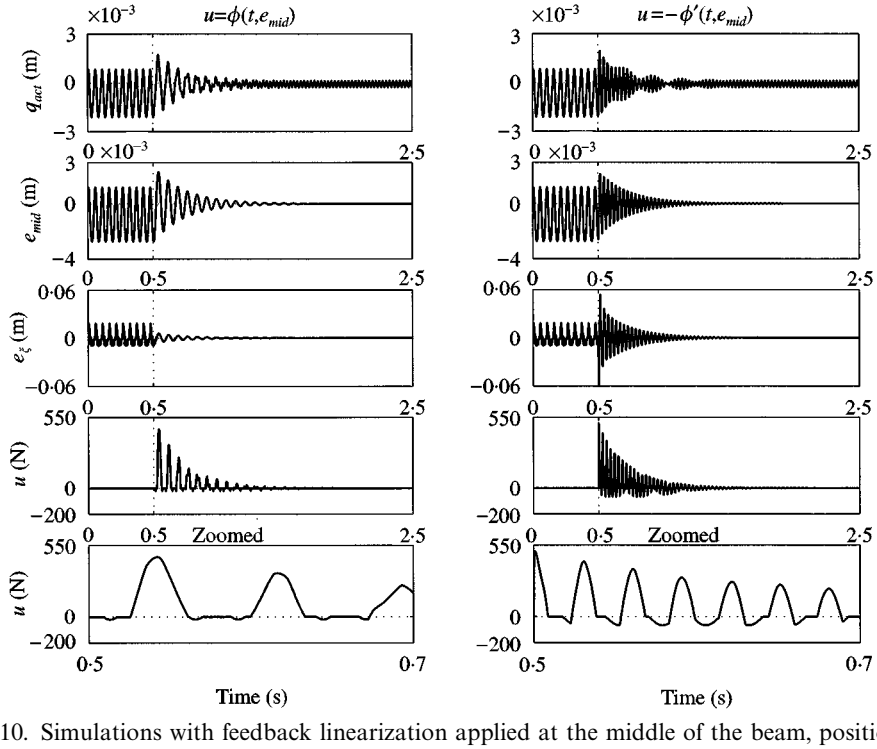

Figure 10. Simulations with feedback linearization applied at the middle of the beam, position 67.

matrix B is equal in both error schemes. However, the error scheme based on $\phi'(t, e_{mid})$ results in a high frequent input, which is caused by adding the stiffness of the one-sided spring k_{nl} to the linear stiffness matrix $\mathbf{K}$; see equation (37). The input u can be kept zero part of the time which can be seen for both control schemes in the lower part of Figure 10.

Partial feedback linearization applied elsewhere on the beam guarantees global asymptotic stability for the actuator d.o.f: $e_{act} = \dot{e}_{act} = 0$. The behaviour of the other d.o.f.s is eventually described by the zero dynamics. The stability of the zero dynamics determines whether vibration amplitudes are reduced and whether the control effort converges to zero. For actuator positions between position 2 and position 50, stability can only be guaranteed locally; see the right part of Figure 9. The ability to stabilize the 1-periodic solution based only on the local asymptotic stability of the zero dynamics, is shown by simulations as depicted in Figure 11 with the input u based on equations (30) and (31). The simulations are performed with an actuator placed at a quarter of the beam, position 34; see Figure 1. At this actuator position, the 1-periodic solution at 35 Hz is stabilized after control is switched on at $t = 0{\cdot}5$ s. Once the d.o.f. at the actuator position vibrates in the 1-periodic response, at $t = 0{\cdot}8$ s, the behaviour of the other d.o.f.s is described by the zero dynamics. The stability of the zero dynamics is illustrated in Figure 11, where it can be seen that the errors e_{mid} and e_ξ converge to zero. As the errors converge to zero, the control effort decreases. The error convergence of the zero dynamics is independent of the control parameters: $K_P = 10^4/\text{s}^2$ and $K_D = 100/\text{s}$.

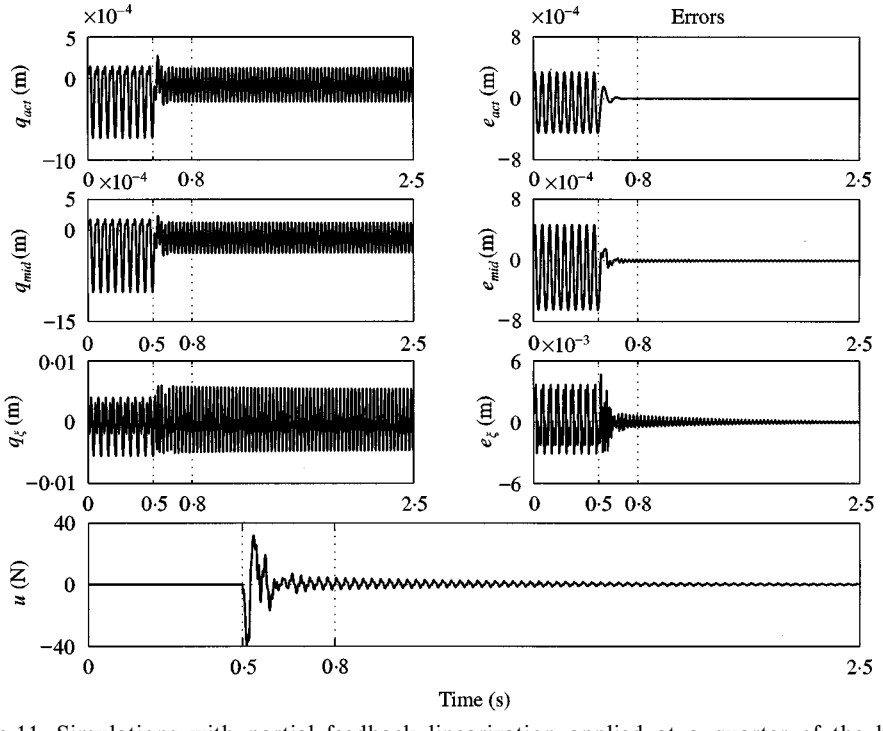

Figure 11. Simulations with partial feedback linearization applied at a quarter of the beam, position 34.

Experiments with partial feedback linearization and an actuator placed at a quarter of the beam, position 34, show a similar behaviour as compared to the simulations which can be seen in Figure 12. In the upper part of Figure 12, the displacements at the actuator position q_{act} and at the middle of the beam q_{mid} are depicted. Both displacements are measured with linear variable differential transformers (LVDTs) having an accuracy of $\approx 10^{-6}$ m. Up to $t = 0{\cdot}5$ s, the uncontrolled system vibrates in the stable 2-periodic response with large-amplitude vibration. At $t = 0{\cdot}5$ s, control is switched on after which the 1-periodic solution is stabilized giving both a vibration amplitude reduction and a control effort that converges to zero. The input u accounts for the main difference between experiment and simulation as can be seen in the lower part of Figure 12. This difference is due to the generation of the control force by a shaker amplifier combination. The shaker-amplifier combination contains mechanical and electrical parts that are being modelled accurately only within a limited frequency range; for practical reasons a restriction is made to a third order model [22]. Besides the shaker-amplifier combination, some other error sources ought to be mentioned, namely inaccuracy in the measured displacements (q_{mid}, q_{act}), accelerations ($\ddot{q}_{mid}$, $\ddot{q}_{act}$), and forces (u, $v(t)$), inaccuracy in the state reconstruction of the velocities ($\dot{q}_{act}$, $\dot{q}_{mid}$) and the state variables of the virtual d.o.f. (ξ, $\dot{\xi}$, $\ddot{\xi}$), inaccuracy by limiting the number of d.o.f.s in the model of the beam, inaccuracy in the approximation of the 1-periodic solution needed as the desired trajectory for control, and inaccuracy in the model of the one-sided spring which is constructed as a second beam and which is modelled by only considering its static behaviour [22].

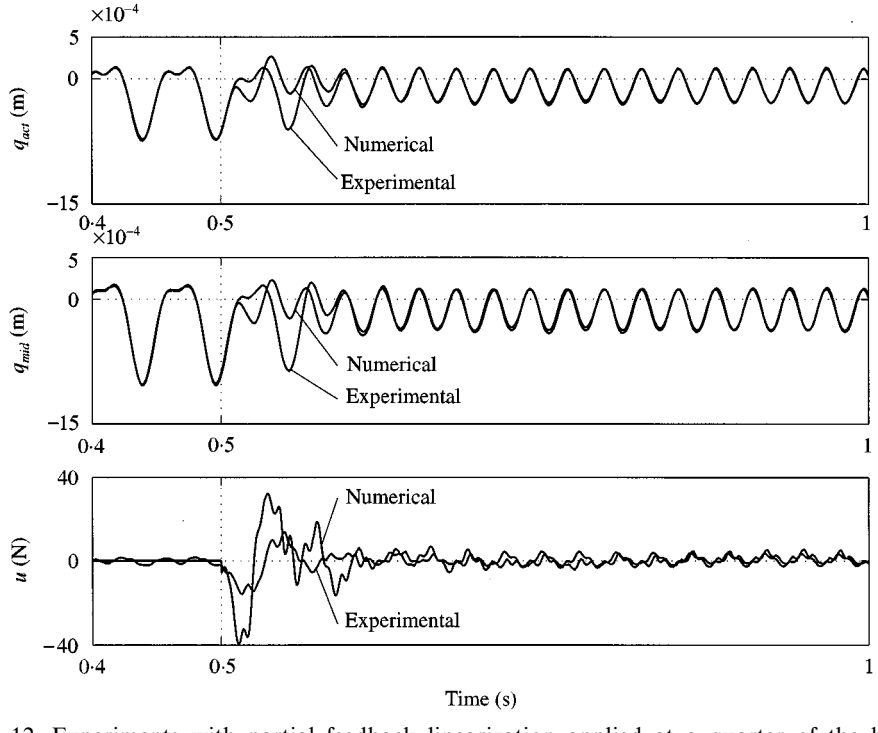

Figure 12. Experiments with partial feedback linearization applied at a quarter of the beam, position 34.

8. CONCLUSIONS

Stabilizing the 1-periodic solution of a harmonically excited beam with one-sided spring can reduce harmful vibration amplitudes whereas the control effort needed converges to zero. The 1-periodic solution is stabilized with non-linear control based on feedback linearization. Feedback linearization applied at the middle of the beam guarantees global asymptotic stability of the entire error dynamics while the control effort can be kept zero part of the time. Partial feedback linearization applied elsewhere on the beam guarantees global asymptotic stability of the d.o.f. at the actuator position. The behaviour of the other d.o.f.s is described by the zero dynamics once the errors at the actuator position tend to zero. The stability of the zero dynamics determines whether vibration amplitudes are reduced for the entire beam. The global asymptotic stability of the zero dynamics can be guaranteed for a limited range of actuator positions applying the circle criterion. At the other actuator positions only local asymptotic stability can be obtained at certain regions for the excitation frequency. However, local asymptotic stability of the zero dynamics can be sufficient to stabilize the 1-periodic solution of the beam system as shown by simulations and experiments.

Further research is focussed on a control scheme based on linear error feedback [9]. Linear error feedback does not globally asymptotically stabilize the error of a particular d.o.f. but modifies the entire error dynamics by adding damping or stiffness such that the entire error can become stable at the origin. In this way, the input u can be chosen just large enough to guarantee local or global asymptotic stability, respectively, which is expected to reduce the required control effort.

REFERENCES

1. S. H. Doole and S. J. Hogan 1996 *Dynamics and Stability of Systems* **11**, 19–47. A piecewise linear suspension bridge model: nonlinear dynamics and orbit continuation.
2. F. Pfeiffer and A. Kunert 1990 *Nonlinear Dynamics* **1**, 63–74, Rattling models from deterministic to stochastic processes.
3. R. Bishop 1994 *Philosophical Transactions of the Royal Society London* **347**, 347–351. Impact oscillators.
4. G. Chen and X. Dong 1993 *International Journal of Bifurcation and Chaos* **3**, 1363–1409. From chaos to order—Perspectives and methodologies in controlling chaotic nonlinear dynamical systems.
5. T. Shinbrot 1995 *Advances in Physics* **44**, 73–111. Progress in the control of chaos.
6. E. Ott, C. Grebogi and J. A. Yorke 1990 *Physical Review Letters* **64**, 1196–1199. Controlling chaos.
7. T. L. Vincent 1997 *IEEE Control Systems Magazine* 65–76. Control using chaos.
8. G. Baker, F. A. McRobie and J. M. T. Thompson 1997 *Proc Instn Mech Engrs* **211**, 349–363. Implications of chaos theory for engineering science.
9. M. F. Heertjes and M. J. G. van de Molengraft 1998 *Proceedings of the* 4*th Nonlinear Control Systems Design Symposium*, 47–52. *Enschede*, *NOLCOS*'98: *IFAC*. Global stabilization of the 1-periodic response of a beam with one-sided spring.
10. M. F. Heertjes, M. J. G. van de Molengraft, J. J. Kok and D. H. van Campen 1997 *Dynamics and Control* **7**, 361–375. Vibration reduction of a harmonically excited beam with one-sided spring using sliding computed torque control.
11. J.-J. E. Slotine and W. Li 1991 *Applied Nonlinear Control*. New York: Prentice-Hall.

12. M. W. Spong 1995 *IEEE Control Systems Magazine* 49–55. The swing up control problem for the acrobot.
13. G. A. Leonov, D. V. Ponomarenko and V. B. Smirnova 1996 *Frequency-Domain Methods for Nonlinear Analysis—Theory and Applications*, Singapore: World Scientific.
14. S. W. Shaw and P. J. Holmes 1983 *Journal of Sound and Vibration* **90**, 129–155. A periodically forced piecewise linear oscillator.
15. H. Y. Hu 1995 *Acta Mechanica Sinica* **11**, 251–258. Controlling chaos of a periodically forced nonsmooth mechanical system.
16. R. R. Craig Jr. 1985 *Combined Experimental/Analytical Modeling of Dynamic Structural Systems* (D. R. Martinez and A. K. Miller, editors), **AMD-67**, 1–30. New York: ASME. A review of time-domain and frequency-domain component mode synthesis method.
17. R. H. B. Fey, D. H. van Campen and A. de Kraker 1996 *ASME Journal of Vibration and Acoustics* **118**, 147–153. Long term structural dynamics of mechanical systems with local nonlinearities.
18. T. Yoshizawa 1975 *Stability Theory and the Existence of Periodic Solutions and Almost Periodic Solutions*. New York: Springer-Verlag.
19. H. K. Khalil 1996 *Nonlinear Systems*. Englewood Cliffs, Prentice-Hall, second edition.
20. T. S. Parker and L. O. Chua 1989 *Practical Numerical Algorithms for Chaotic Systems*. New York: Springer-Verlag.
21. F. C. Moon 1987 *Chaotic Vibrations*: *An Introduction for Applied Scientists and Engineers*. New York: John Wiley & Sons.
22. M. F. Heertjes and M. J. G. van de Molengraft 1998 *Proceedings of the 4th Nonlinear Control Systems Design Symposium*, 569–574. *Enschede*, *NOLCOS*'98: *IFAC*. Stabilizing the 1-periodic response of a beam with one-sided spring; experiment versus simulation.

APPENDIX A

For an actuator placed at a quarter of the beam, position 34, the following matrices were used:

$$\mathbf{M} = \begin{bmatrix} 2{\cdot}49171266\times10^{0} & -7{\cdot}39353071\times10^{-1} & -1{\cdot}00670592\times10^{-2} \\ -7{\cdot}39353071\times10^{-1} & 4{\cdot}70207355\times10^{0} & 2{\cdot}55145832\times10^{-2} \\ -1{\cdot}00670592\times10^{-2} & 2{\cdot}55145832\times10^{-2} & 2{\cdot}78179792\times10^{-4} \end{bmatrix} \text{(kg)},$$

$$\mathbf{B} = \begin{bmatrix} 9{\cdot}13975994\times10^{1} & -5{\cdot}46796875\times10^{1} & -3{\cdot}12421552\times10^{-1} \\ -5{\cdot}46796875\times10^{1} & 7{\cdot}30340017\times10^{1} & 3{\cdot}54360794\times10^{-1} \\ -3{\cdot}12421552\times10^{-1} & 3{\cdot}54360794\times10^{-1} & 1{\cdot}08926256\times10^{-2} \end{bmatrix} \text{(Ns/m)},$$

$$\mathbf{K} = \begin{bmatrix} 3{\cdot}82896231\times10^{5} & -2{\cdot}59390789\times10^{5} & 9{\cdot}78184925\times10^{-8} \\ -2{\cdot}59390789\times10^{5} & 2{\cdot}10586254\times10^{5} & -2{\cdot}65589609\times10^{-7} \\ 9{\cdot}78184925\times10^{-8} & -2{\cdot}65589609\times10^{-7} & 6{\cdot}10747501\times10^{1} \end{bmatrix} \text{(N/m)},$$

$k_{nl} = 1{\cdot}9656\times10^{5}$ (N/m),

$A_{exc} = 9{\cdot}398\times10^{-4}\,(2\pi f_{exc})^{2}$ (N).